Coherent Control in the Presence of Intrinsic Decoherence: Proton Transfer in Large Molecular Systems

Victor S. Batista
Department of Chemistry, Yale University, New Haven, Connecticut 06520-8107

Paul Brumer
Chemical Physics Theory Group, Department of Chemistry, and Photonics Research Ontario, University of Toronto, Toronto, Ontario, Canada M5S 3H6

(Received 17 March 2002; published 17 September 2002)

An efficient semiclassical approach is developed and used to calculate the coherent-control map and time dependent decoherence measure for the excited-state proton transfer dynamics associated with the keto-enolic tautomerization reaction of 2-(2′-hydroxyphenyl)-oxazole. The method extends the usual bichromatic coherent-control scenario to simulate control at finite times after photoexcitation of the system. Extensive coherent control is demonstrated in a large molecule despite the ultrafast decoherence phenomena, providing results of broad theoretical and experimental interest.

DOI: 10.1103/PhysRevLett.89.143201 PACS numbers: 34.30.+h, 03.65.Sq, 03.65.Yz

Understanding the role of quantum coherences in intramolecular relaxation processes of large molecules is a subject of great interest [1–3]. In such systems (e.g., biological molecules), the relevant dynamics often involves the motion of a molecular subcomponent and the remainder of the molecule acts to decohere the dynamics [4]. Experimental studies have thus far aimed at elucidating the nature of such type of dynamics in an effort to understand its coherence properties. In this Letter, we computationally demonstrate the possibility of coherently controlling [5,6] such systems. In addition to the obvious advance associated with demonstrating control, this approach also provides a technique for significantly advancing our understanding of the role of coherent quantum mechanics in the dynamics of these ubiquitous relaxation processes.

Coherent control [5,6] exploits the coherence properties of lasers to encode and manipulate quantum mechanical interferences in matter. Several coherent-control scenarios have been demonstrated both computationally and experimentally for simple reactions in small molecules [5]. The possibility of significantly controlling intramolecular dynamics in large molecular systems, however, has often been deemed to be unrealistic due to the deleterious effects of rapid decoherence. In this Letter, we develop and implement a semiclassical method to explore quantum control in large molecules, and we demonstrate that quantum control is achievable even in the presence of ultrafast decoherence. The new computational approach builds upon previous work [7–9] and involves a semiclassical initial value representation that provides an explicit description of all degrees of freedom in the system. The method is applied to simulations of coherent control of the excited-state intramolecular proton transfer in 2-(2′-hydroxyphenyl)-oxazole. The reaction is shown in Fig. 1.

The system is described by a full-dimensional model Hamiltonian [7] that includes 35 coupled degrees of freedom and 16 out-of-the-plane vibrational modes that are approximately decoupled from the reaction coordinate. The potential was computed [7] at the configuration interaction with singlet excitations level using GAUSSIAN94. The system is prepared in an initial coherent superposition state on the ground electronic state:

$$|\Psi_0\rangle = c_1 |1\rangle + c_2 |2\rangle, \tag{1}$$

where $|i\rangle$ is a nuclear eigenstate of energy E_i. This superposition state is photoexcited by two monochromatic laser pulses with a total electric field $\boldsymbol{\epsilon}(t)$:

$$\boldsymbol{\epsilon}(t) = F_1(t - t_1)\boldsymbol{\epsilon}_1 e^{-i(\omega_1 t+\theta_1)} + F_2(t - t_2)\boldsymbol{\epsilon}_2 e^{-i(\omega_2 t+\theta_2)} + \text{c.c.}, \tag{2}$$

where $\boldsymbol{\epsilon}_j = \epsilon_j \hat{\boldsymbol{\epsilon}}$, $j = 1, 2$ are time independent real vectors, and c.c. denotes the complex conjugate of the preceding terms. The functions F_j in Eq. (2) describe the pulse shapes, and θ_j are the phases of the two pulses. Hence, in this pulsed laser variant of cw bichromatic coherent control [5], the superposition of $|1\rangle$ and $|2\rangle$ are photoexcited by the laser field with frequencies ω_1 and

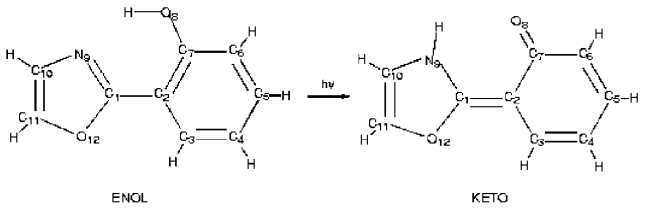

FIG. 1. Molecular structural diagram describing the excited-state intramolecular proton transfer reaction in 2-(2′-hydroxyphenyl)-oxazole.

 0031-9007/02/89(14)/143201(4)$20.00

ω_2. The states created by the two photoexcitation routes interfere with one another, and these quantum mechanical interferences affect the time dependent reactant population $P(t)$ of the proton. Here $P(t)$ is defined as

$$P(t) \equiv \langle \Psi_t \mid R \mid \Psi_t \rangle, \tag{3}$$

where R is a function of the proton coordinate that is zero on the product side of a dividing surface in configuration space and unity on the reactant side. Assuming that the field is sufficiently weak to allow the use of first order perturbation theory, we obtain the time-evolved wave function $\mid \Psi_t \rangle$ as

$$\mid \Psi_t \rangle = -\frac{i}{\hbar} \sum_{j=1}^{2} c_j \int_{-\infty}^{t} dt' \left[\sum_{k=1}^{2} \epsilon_k e^{-i[(E_j+\hbar\omega_k)t'/\hbar+\theta_k]} \right] F_k(t'-t_k)] e^{-i\hat{H}(t-t')/\hbar} \hat{\boldsymbol{\epsilon}} \cdot \boldsymbol{\mu} \mid j \rangle, \tag{4}$$

where $\hat{H}$ is the Hamiltonian on the excited electronic surface, $\boldsymbol{\mu}$ is the electric dipole operator and where only the near resonant terms have been retained (the rotating wave approximation). Substituting Eq. (4) into Eq. (3), we obtain the time dependent reactant population in the weak field limit,

$$\begin{aligned} P(t) = \hbar^{-2} \int_{-\infty}^{t} dt' \int_{-\infty}^{t} dt'' \sum_{j,j'=1}^{2} c_j c_{j'}^{*} \langle j' \mid \hat{\boldsymbol{\epsilon}} \cdot \boldsymbol{\mu} e^{i\hat{H}(t-t'')/\hbar} \mathrm{Re}^{-i\hat{H}(t-t')/\hbar} \hat{\boldsymbol{\epsilon}} \cdot \boldsymbol{\mu} \mid j \rangle \\ \times e^{i(E_{j'}t''-E_j t')/\hbar} \epsilon_1^2 [F_1(t'-t_1)F_1(t''-t_1)e^{i\omega_1(t''-t')} \ast F_2(t'-t_2)F_2(t''-t_2)x^2 e^{i\omega_2(t''-t')} + F_2(t'-t_2)F_1(t''-t_1) \\ \times x e^{i[(\omega_1 t''-\omega_2 t')+\Theta]} + F_1(t'-t_1)F_2(t''-t_2)x e^{i[(\omega_2 t''-\omega_1 t')-\Theta]}], \end{aligned} \tag{5}$$

as a function of the laser controllable parameters $x = \epsilon_2/\epsilon_1$ and $\Theta = \theta_1 - \theta_2$. Note that Eq. (5) contains terms in $|c_j|^2$ corresponding to direct contributions, as well as terms in $c_j c_{j'}^{*}$ that correspond to interference terms. Hence, by altering the c_j, we can control the interference term, and, hence, the dynamics.

Equation (5) requires the exact quantum propagation of the system, a computational task that becomes daunting, if not intractable, for systems with more than 6 degrees of freedom (e.g., a molecule with four atoms). We therefore replace the time evolution operators by the coherent state expression in the initial value representation (IVR) [10]. That is,

$$\begin{aligned} e^{-i\hat{H}t/\hbar} = (2\pi\hbar)^{-N} \int d\mathbf{p}_0 \int d\mathbf{q}_0 e^{iS_t(\mathbf{p}_0,\mathbf{q}_0)/\hbar} C_t(\mathbf{p}_0,\mathbf{q}_0) \\ \mid g_{\mathbf{q}_t,\mathbf{p}_t} \rangle \langle g_{\mathbf{q}_0,\mathbf{p}_0} \mid, \end{aligned} \tag{6}$$

where $\mid g_{\mathbf{q},\mathbf{p}} \rangle$ is a coherent state. The integration variables $(\mathbf{p}_0, \mathbf{q}_0)$ in Eq. (6) are the initial conditions for classical trajectories and $\mathbf{q}_t \equiv \mathbf{q}_t(\mathbf{p}_0, \mathbf{q}_0)$ and $\mathbf{p}_t \equiv \mathbf{p}_t(\mathbf{p}_0, \mathbf{q}_0)$ are the time-evolved nuclear coordinates and momenta. The classical action $S_t(\mathbf{p}_0, \mathbf{q}_0)$ along this trajectory is obtained by integrating the equation,

$$\dot{S}_t = \mathbf{p}_t \cdot \dot{\mathbf{q}}_t - H(\mathbf{p}_t, \mathbf{q}_t), \tag{7}$$

along with Hamilton's equations of motion for $\mathbf{p}_t$ and $\mathbf{q}_t$. Here, $H(\mathbf{q}, \mathbf{p})$ is the full-dimensional model Hamiltonian [7] that explicitly describes the motion of all degrees of freedom in the system. The preexponential factor $C_t(\mathbf{p}_0, \mathbf{q}_0)$, introduced in Eq. (6), involves the monodromy matrix elements that are propagated in accord with Ref. [7].

Substituting Eq. (6) into Eq. (5) gives the semiclassical IVR for $P(t)$:

$$\begin{aligned} P(t) = \hbar^{-2}(2\pi\hbar)^{-2N} \int d\mathbf{p}_0 \int d\mathbf{q}_0 \int d\mathbf{p}_0' \int d\mathbf{q}_0' \int_{-\infty}^{t} dt' \int_{-\infty}^{t} dt'' \sum_{j,j'} c_j c_{j'}^{*} \\ \times e^{i(S_{t-t'}(\mathbf{p}_0,\mathbf{q}_0)-S_{t-t''}(\mathbf{p}_0',\mathbf{q}_0'))/\hbar} C_{t-t'}(\mathbf{p}_0,\mathbf{q}_0) C_{t-t''}^{*}(\mathbf{p}_0',\mathbf{q}_0') \times \langle j' \mid \mathbf{p}_0', \mathbf{q}_0' \rangle \langle \mathbf{p}_{t-t''}', \mathbf{q}_{t-t''}' \mid R \mid \mathbf{p}_{t-t'}, \mathbf{q}_{t-t'} \rangle \langle \mathbf{p}_0, \mathbf{q}_0 \mid j \rangle \\ \times e^{i(E_{j'}t''-E_j t')/\hbar} \epsilon_1^2 [F_1(t'-t_1)F_1(t''-t_1)e^{i\omega_1(t''-t')} + F_2(t'-t_2)F_2(t''-t_2)x^2 e^{i\omega_2(t''-t')} + F_2(t'-t_2)F_1(t''-t_1) \\ \times x e^{i[(\omega_1 t''-\omega_2 t')+\Theta]} + F_1(t'-t_1)F_2(t''-t_2)x e^{i[(\omega_2 t''-\omega_1 t')-\Theta]}]. \end{aligned} \tag{8}$$

As an example, we consider the case where the initial superposition state [Eq. (1)] involves state $|1\rangle$ as the ground vibrational state of the internal oxazole-hydroxyphenyl in-the-plane bending mode—i.e., bending motion of the $C_1C_2C_7$ angle (Fig. 1), and state $|2\rangle$ as the first excited state associated with this vibrational mode. In addition, $c_j = c_k = 1/\sqrt{2}$, and the temporal profiles of the laser pulses are Gaussian; $F_1(t-t_1) = F_2(t-t_2) = (\beta/\pi)^{1/4} \exp(-\beta t^2/2)$, where $\beta = 2\ln(2)/25\ \mathrm{fs}^{-1}$ and $t_1 = t_2 = 0$. Hence, the FWHM of the pulse is chosen to be 25 fs, and ω_1 and ω_2 are taken

as 324.7 and 327.8 nm, respectively. Because of the fact that the semiclassical propagator does not preserve the norm of the time-evolved wave function, percentages of reactant are reported in Figs. 2 and 3, normalized according to $100 \times \langle \Psi_t \mid R \mid \Psi_t \rangle / \langle \Psi_t \mid \Psi_t \rangle$. Such normalized expression is independent of ϵ_1.

Substituting these conditions into the semiclassical initial value representation (SC-IVR) approximation of $P(t)$ gives a "direct" SC-IVR approach for computations of bichromatic coherent control at *finite* times after photoexcitation of the system [i.e., an approach that computes $P(t)$, as a function of the pulse phases and intensities, without having to store or compute any other intermediate quantities]. The efficiency of the method relies on the partial cancellation of phases that results from the forward-backward aspect of the calculation, where the product of the two time evolution operators in Eq. (5) is treated as *one* evolution operator [7]. This phase cancellation effect is combined with the "smoothing" effect associated with the *time average* over nuclear motion, introduced by the time integrals in Eq. (8). Time integrals are computed through Monte Carlo sampling of propagation times $(t - t')$ and $(t - t'')$, in accord with the distribution functions introduced by the intensity profiles F_1 and F_2, respectively. Thus, the presence of a pulse of finite (as opposed to delta function) duration significantly aids in the convergence of the semiclassical method. The preexponential factor $C_t(\mathbf{p}_0, \mathbf{q}_0)$, in Eq. (8) is computed by the approximate version of the semiclassical initial value representation method developed in Ref. [11], as implemented in Ref. [7]. The method is specifically designed to avoid the computational bottleneck for applications of the SC-IVR to large molecular systems, which is caused by the calculation of the monodromy matrix elements involved in the preexponential factor of the semiclassical amplitude.

Note that we choose a specific pulse shape, as opposed to the pulse shaping approach of optimal control techniques [6]. Doing so allows us to simultaneously explore all possible outcomes that result from different initial superpositions of the initial state. Similarly, the experimentalist need only determine a few data points which, in conjunction with Eq. (8), determine the control map, i.e., control as a function of the control parameters Θ and $S = x^2/(1 + x^2)$.

Figure 2 shows a contour plot of the percentage enol form (i.e., the reactant) at 100 fs after photoexcitation of the system. The coherent-control map (Fig. 2) indicates that the percentage reactant drastically changes as a function of the relative pulse laser parameter Θ. That is, there is a broad range of yield control over an extended range of S. Maximum control is attained in the $0.25 < S < 0.55$ range, where the percentage of the enol tautomer can be varied from more than 80% to less than 20%, by varying Θ from 0° to ~210°. Note that these large changes are achieved solely by changing the relative *phases* of the photoexcitation pulses that populate the electronic excited state by creating an initial coherent superposition. Similar control persists at larger values of S, where the percentage reactant can be reduced from more than 80% to less than 30% by changing Θ from 0° to ~120°. Figure 3 shows contour plots of the percentage product yields at 200 fs after excitation of the system. Here, the degree of yield control is maximum in the $0.2 < S < 0.8$ range, where the reactant probability can be reduced from more 80% to less than 40% by changing Θ from 120°–180° to 0°.

The extent to which these results are significant is associated with the advent of intrinsic decoherence experienced by the proton during the course of the dynamics. To this end, we examine the time dependence of $\mathrm{Tr}[\rho^2(t)]$, where $\rho(t)$ is the one-particle *reduced* density matrix

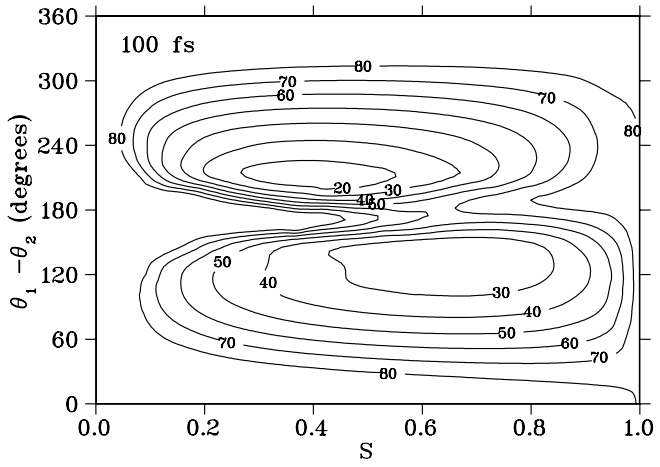

FIG. 2. Contour plot of the percentage reactant for bichromatic coherent control at 100 fs after photoexcitation of the system.

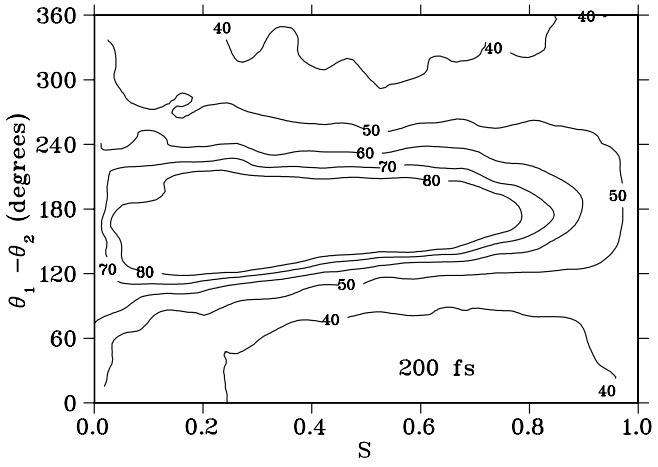

FIG. 3. Contour plot of the percentage reactant for bichromatic coherent control at 200 fs after photoexcitation of the system.

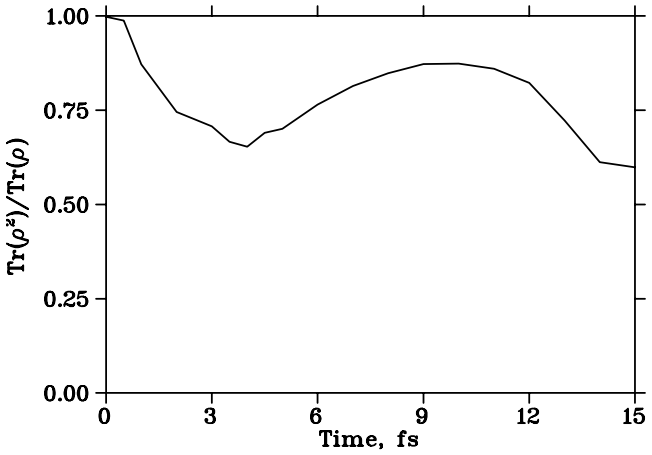

FIG. 4. Trace of ρ^2 as a function of time during the first 15 fs of dynamics after photoexcitation of the system.

associated with the proton, which serves as a decoherence measure [12–15]. Further, we choose the initial state as the Gaussian ground vibrational state of the stretching mode associated with the OH bond (see Fig. 1) promoted to the first electronically excited state. Since the decoherence rate is expected [15] to increase with the configuration space size of the $\rho(0)$, this choice of initial condition should provide an approximate lower bound to the rate. Initially, $\mathrm{Tr}[\rho(0)^2] = 1$, indicative of a pure state. As the reaction proceeds, the proton becomes coupled to the remaining degrees of freedom in the system (i.e., a bath of 34 coupled modes) and $\mathrm{Tr}(\rho^2)$ is expected to decay.

Figure 4 shows $\mathrm{Tr}(\rho^2)$ as computed during the first 15 fs of dynamics. During this short time, more than 98% of the population remains on the reactant side [7]. However, $\mathrm{Tr}(\rho^2)$ decays to $\sim$0.6 by 4 fs (a time scale comparable to one-half the period of the OH stretch in the enol tautomer). At this time, the slope of the curve changes sign, indicating a change of the underlying physical process. Additional computations at longer times, specifically at 100 and 200 fs, show a further decrease of $\mathrm{Tr}(\rho^2)$ to 0.54 and 0.38, respectively. This is consistent with the fact that by 200 fs over 13% of the H-atom population has been transferred and that comparisons with fewer degree of freedom models [7] show that the dynamics beyond 100 fs involves coupling to a significant number of background modes. Figures 2 to 3 make clear that extensive coherent control is taking place in a system despite the ongoing decoherence.

It is important to note that these are benchmark state-of-the-art computations. Each time reported in Fig. 4 requires a separate calculation of a 140-dimensional integral using $\approx 10^7$ semiclassical trajectories. This considerable computational effort aims to produce the first explicit calculations of coherent control in a system with many coupled degrees of freedom. To the best of our knowledge, our computations also constitute the first explicit calculations of a decoherence measure in a system with many degrees of freedom.

In summary, we have demonstrated wide-ranging bichromatic coherent control in a large molecule despite ultrafast intrinsic decoherence. The predicted range of control is extensive, providing results of broad theoretical and experimental interest.

V. S. B. acknowledges a generous allocation of supercomputing time from the National Energy Research Scientific Computing Center (NERSC) and financial support for this work from the Provost's office, Yale University. P. B. gratefully acknowledges financial support from the U.S. Office of Naval Research and Photonics Research Ontario.

[1] R. W. Schoenlein, L. A. Peteanu, R. A. Mathies, and C. V. Shank, Science **254**, 412 (1991).
[2] Q. Wanf, R. W. Schoenlein, L. A. Peteanu, R. A. Mathies, and C. V. Shank, Science **266**, 422 (1994).
[3] C. A. Chatzidimitriou-Dreismann, T. Abdul-Redah, and J. Sperling, J. Chem. Phys. **113**, 2784 (2000).
[4] We refer to such a decoherence process as "intrinsic decoherence" to make a distinction from cases where decoherence is caused by coupling to an external bath.
[5] M. Shapiro and P. Brumer, in *Advances in Atomic, Molecular and Optical Physics*, edited by B. Bederson and H. Walther (Academic, San Diego, 2000), pp. 287–343.
[6] S. A. Rice and M. Zhao, in *Optical Control of Molecular Dynamics* (Wiley, New York, 2000).
[7] V. Guallar, V. S. Batista, and W. H. Miller, J. Chem. Phys. **113**, 9510 (2000).
[8] V. S. Batista and P. Brumer, J. Chem. Phys. **105**, 2591 (2001).
[9] V. S. Batista and P. Brumer, J. Chem. Phys. **114**, 10 321 (2001).
[10] M. F. Herman and E. Kluk, Chem. Phys. **91**, 27 (1984).
[11] V. Guallar, V. S. Batista, and W. H. Miller, J. Chem. Phys. **110**, 9922 (1999).
[12] P. C. Lichtner and J. J. Griffin, Phys. Rev. Lett. **37**, 1521 (1976).
[13] X.-P. Jiang and P. Brumer, Chem. Phys. Lett. **208**, 179 (1993).
[14] S. Habib, W. H. Zurek, and J. P. Paz, Phys. Rev. Lett. **70**, 1187 (1993).
[15] A. Pattanayak and P. Brumer, Phys. Rev. Lett. **79**, 4131 (1997).